Clinical, Cosmetic and Investigational Dermatology

Dovepress

open access to scientific and medical research

Open Access Full Text Article

ORIGINAL RESEARCH

Human Adipose-Derived Mesenchymal Stem Cells-Derived Exosomal microRNA-19b Promotes the Healing of Skin Wounds Through Modulation of the CCL1/TGF-β Signaling Axis

This article was published in the following Dove Press journal:
Clinical, Cosmetic and Investigational Dermatology

Guoxiu Cao[1]
Bei Chen[2]
Xian Zhang[3]
Hongyun Chen[1]

[1]Department of Dermatology, The Third Affiliated Hospital of Zunyi Medical University (The First People's Hospital of Zunyi), Zunyi, Guizhou 563000, People's Republic of China; [2]Department of Pharmacy, The Third People's Hospital of Zunyi, Zunyi, Guizhou 563000, People's Republic of China; [3]Department of Project, MDL Biotech. Co.Ltd, Beijing 100080, People's Republic of China

Introduction: Human adipose-derived mesenchymal stem cells (ADMSCs) with their secretory factors are able to induce collagen synthesis and fibroblast migration in the wound healing process. This study is launched to figure out the effect of human ADMSCs-derived exosomes on skin wound healing.

Methods: ADMSCs were extracted and ADMSCs-derived exosomes were identified. Skin damage models were established by treating HaCaT cells and human skin fibroblasts with H_2O_2. Next, the roles of ADMSCs and their derived exosomes were investigated. The exosomal miRNA then was analyzed, and the function of miRNA on the H_2O_2-induced cells was studied by miRNA suppression. Bioinformatics analysis, luciferase activity and RIP assays were implemented to find the target genes ofthe miRNA and the modulated pathways. A mouse skin damage model was induced to elucidate the effects of exosomes in vivo by injecting exosomes.

Results: H_2O_2 treatment significantly reduced the viability of HaCaT cells and increased their apoptosis rate. Co-culture with ADMSCs or their derived exosomes could improve the cell damage caused by H_2O_2. Meanwhile, H_2O_2 treatment promoted the internalization of exosomes. ADMSCs and their derived exosomes significantly increased miR-19b expression in the recipient cells, while inhibiting miR-19b resulted in a reduction in the therapeutic effect of ADMSCs-derived exosomes. Besides, miR-19b regulated the TGF-β pathway by targeting CCL1. The therapeutic effect of exosomes was further confirmed by a mouse model of skin damage.

Conclusion: Our study indicates that exosomal miR-19b derived from ADMSCs regulates the TGF-β pathway by targeting CCL1, thereby promoting the healing of skin wounds.

Keywords: human adipose-derived mesenchymal stem cells, exosome, microRNA-19b, healing of skin wounds, CCL1, TGF-β signaling pathway

Introduction

The skin, including the dermis (deeper layer) and epidermis (surface layer), is the biggest barrier between the external environment and the human body.[1] Skin injuries are the commonest type of injuries in daily life.[2] There are many different causes of skin wound, such as incision, burn, and blunt force, while all of these wounds trigger an immune response.[3] Skin wound may lead to difficulties in excessive scarring or in healing,[4] and improper treatment can lead to pain,

Correspondence: Hongyun Chen
Email Chenhongyuan4242@163.com

submit your manuscript | www.dovepress.com
DovePress
http://doi.org/10.2147/CCID.S274370

infection, and bad sequelae such as adhesions.[5] Skin wound healing is a dynamic process that coordinates a battery of complex processes implicated in tissue repair, such as hemostasis, cell proliferation, inflammation and remodeling.[6] Despite these significant findings, extracellular cues or specific signaling pathways that coordinate the complex network of healing processes remain unclear.[7] Thus, there is an urgent need to explore a way for promoting skin wound healing.

Human adipose-derived mesenchymal stem cells (ADMSCs) are demonstrated to be significant factors for the regenerative process post tissue injury.[8] ADMSCs have been applied in the therapy of defects and scars in soft tissues, and burn injuries, which could improve the quality of wound healing process.[9] Exosomes, a type of small lipid bilayer vesicle with a diameter of 30–150 nm are derived from certain biological fluids, including blood, saliva, urine, synovial fluid, amniotic fluid and pleural fluid or secreted by most cells.[10] A study has discussed that human bone marrow MSCs-secreted exosomes stimulated by deferoxamine accelerate cutaneous wound healing via expediting angiogenesis.[11] Another study has demonstrated that ADMSC-exosomes can be considered as a new promising cell-free treatment for atopic dermatitis.[12] MicroRNAs (miRs) are a class of small non-coding single-stranded RNAs consisting of approximately 19–22 nucleotides.[13] A study has demonstrated that miR-21 improved age-associated skin wound healing defects in mice.[14] Another study has presented that miR-19b-3p suppressed inflammatory injury and extracellular matrix degradation in chondrocytes.[15] A more recent report established that the depletion of miR-19a/b contributes to sustained inflammation and impaired healing in chronic wounds.[16] Interestingly, miR-19b-3p in exosomes is found to induce NF-κB via direct inhibition of the suppressor of cytokine signaling 1 in the macrophage,[17] proposing the possibility that miR-19b exerted its function through exosomes. Therefore, we postulated that miR-19b is involved in the wound healing process via ADMSCs-derived exosomes. Chemokine CC motif ligand 1 (CCL1), an 8-kDa peptide in the CC chemokine family with the presence of two adjacent cysteines near the amino terminus, has been suggested in the regulation of nociceptive processing.[18] It is reported that up-regulated levels of inflammatory factors such as CCL1 expression inhibited hyperglycaemia and induced an inflammatory response.[19] Moreover, expression of CCL1 was found to be promoted in the acute lesional skin of atopic dermatitis patients relative to their non-lesional skin.[20] Therefore, it is hypothesized in this study that ADMSCs-derived exosomal miR-19b is implicated in skin wound healing process. In addition, we aim to clarify the impact of ADMSCs-derived exosomal miR-19b on skin wound healing process by regulating CCL1.

Materials and Methods

Ethics Statement

All animal experiments were approved by the Animal Ethics Committee of the Third Affiliated Hospital of Zunyi Medical University (Approval number: KY2019-A-26). All animal procedures were implemented in line with the Guide for the Care and Use of Laboratory Animals proposed by National Institutes of Health (NIH Publication No.85–23, revised 1996).

Culture and Identification of ADMSCs

ADMSCs were available from American Type Culture Collection (ATCC, USA, PCS-500-011). The cells were cultivated at 37°C with 5% CO_2 in low-glucose Dulbecco's modified Eagle's medium (DMEM; HyClone, Logan, UT, USA) supplemented with 10% fetal bovine serum (FBS; Gibco) and 0.1% 100 U/mL penicillin-streptomycin. When reaching 70–80% confluence, the cells were detached with 0.25% trypsin (Sigma-Aldrich) and subcultured.

ADMSCs at passage 3 were resuspended in PBS after trypsinization, and the cells were adjusted to 1×10^6 cells/mL. The cell suspension (200 μL) was put into Eppendorf tubes and then probed at 4°C with 5 μL monoclonal antibody for 15 minutes in darkness. The antibodies included CD34 (ab18227), CD44 (ab27285), CD45 (ab27287) and CD105 (ab53318) (all from Abcam, Cambridge, USA) or with appropriate isotype control IgG (Abcam). Excess antibodies were discarded by centrifugation for 5 minutes at 1000 rpm with 2 mL PBS. Afterwards, ADMSCs were resuspended in 400 μL 0.5% paraformaldehyde-contained PBS. Surface markers of ADMSCs were determined by a flow cytometer (FACSCalibur, Becton-Dickinson, Mountain View, CA, USA).

To evaluate the differentiation potentials of ADMSCs, human mesenchymal stem cell osteogenic differentiation medium (CP1202, Weitong Biotechnology Co., Ltd., Shenzhen, Guangdong, China) and adipogenic differentiation medium (CP1211, Weitong Biotechnology) were used for differentiation culture for three weeks or two weeks,

respectively. Alizarin Red staining solution and Oil Red O staining solution were utilized for identification.

Separation and Identification of ADMSCs-Derived Exosomes

ADMSCs were cultured overnight in FBS-free DMEM (Thermo Fisher Scientific, Waltham, MA, USA). The medium was centrifuged at 2000 g for 30 minutes to eliminate cells and debris. The supernatant was transferred to a new test tube and then centrifuged at 100,000 g at 4°C for one hour in an Optima MAX-XP benchtop ultracentrifuge (Beckman Coulter, Inc., Chaska, MN, USA) to generate an exosome precipitate.

The exosomes suspended in PBS were quantified with the application of the bicinchoninic acid (BCA) protein assay kit (Beyotime, Shanghai, China) based upon the manufacturer's protocol. The morphology of exosomes was viewed with a transmission electron microscope (TEM, Tecnai G2 Spirit, FEI, USA). The size distribution of exosomes was confirmed using NanoSight NS300 nanoparticle tracking analysis (NTA, NanoSight Technology, Malvern, UK). In order to detect exosome markers, Western blot assay was performed with CD63 (ab59479, Abcam) and HSP70 (ab181606, Abcam) antibodies.

Reverse Transcription Quantitative Polymerase Chain Reaction (RT-qPCR)

TRIzol reagent (Invitrogen) was utilized for RNA extraction and Reverse Transcription Kits (Invitrogen) for cDNA synthesis. RT-qPCR was implemented by an ABI 7500 Fast Real-Time PCR system referring to the requirements of FastStart Universal SYBR Green Master (Vazyme Biotech Co., Piscataway, NJ, USA). With glyceraldehyde phosphate dehydrogenase (GAPDH) or 5s as the endogenous control, RT-qPCR was conducted for measuring expression of genes. The $2^{-\Delta\Delta CT}$ method was performed for comparative quantification with at least 3 independent experiments. The primer sequences used were as follows:

Human miR-19b: forward primer: 5′-TGCAGGTTT GCATCCAG-3′, reverse primer: 5′- GAACATGTCTG CGTATCTC-3′. Mouse miR-19b: forward primer: 5′-TGCAAATCCATGCAAAACTG-3′, reverse primer: 5′-GAACATGTCTGCGTATCTC-3′. Human CCL1: forward primer: 5′-ACCAGCTCCATCTGCTCCAATG-3′, reverse primer: 5′-TGTGCCTCTGAACCCATCCAAC-3′. Mouse CCL1: forward primer: 5′-GCTTACGGTCTCCAAT AGCTGC-3′, reverse primer: 5′-GCTTTCTCTACCTTTGTT CAGCC-3′. Mouse Bcl-2: forward primer: 5′-CCTGTGG ATGACTGAGTACCTG-3′, reverse primer: 5′-AGCCAG GAGAAATCAAACAGAGG-3′. Mouse Bax: forward primer: 5′-AGGATGCGTCCACCAAGAAGCT-3′, reverse primer: 5′-TCCGTGTCCACGTCAGCAATCA-3′. Mouse interleukin (IL)-6: forward primer: 5′-TACCACTTCACAAG TCGGAGGC-3′, reverse primer: 5′-CTGCAAGTGCATC ATCGTTGTTC-3′. Mouse IL-10: forward primer: 5′-CGGGAAGACAATAACTGCACCC-3′, reverse primer: 5′-CGGTTAGCAGTATGTTGTCCAGC-3′. Human GAPDH: forward primer: 5′-GTCTCCTCTGACTTCAACAGCG-3′, reverse primer: 5′-ACCACCCTGTTGCTGTAGCCAA-3′. Mouse GAPDH: forward primer: 5′-CATCACTGCCACCC AGAAGACTG-3′, reverse primer: 5′-ATGCCAGTGAGCT TCCCGTTCAG-3′. Human or Mouse 5s: forward primer: 5′-CTCGCTTCGGCAGCACAT-3′, reverse primer: 5′-TTTGC GTGTCATCCTTGCG-3′.

A Cell Model of Skin Damage

Human keratinocyte cell line HaCaT (116027, antibody research) and human skin fibroblasts (HSF, CP-H103, Procell, Wuhan, Hubei, China) were cultured in complete Roswell Park Memorial Institute (RPMI)-1640 medium (Gibco) containing 5% FBS (Gibco) and 1% penicillin/streptomycin (ScienCell Research Laboratories, Carlsbad, CA, USA) under the conditions of 37°C and 5% CO_2, and the medium was renewed every 2 days.

As previous described,[21,22] the cell model of skin damage was established. Briefly, cells were induced with H_2O_2 for 12 hours at the varying concentrations of 0 μM, 100 μM, 200 μM, 300 μM, 400 μM, or 500 μM. The effect of H_2O_2 on cell viability and apoptosis level was evaluated by 3-(4,5-dimethylthiazol-2-yl)-2,5-diphenyltetrazolium bromide (MTT) assay and flow cytometry.

MTT Assay

The cell viability was tested by MTT kit (C0009, Beyotime), and the treated cells were cultivated in 96-well plates (5000 cells/well). Ten microliters of MTT solution at 5 mg/mL was appended to each well. The cultures were incubated at 37°C for 4 hours, then mixed well with 100 μL Formazan solution, followed by an incubation at 37°C for another 4 hours. The optical density (OD) value of each well was read at 570 nm wavelength by a microplate reader (Bio-Rad Laboratories, Hercules, CA) to assess cell viability.

Flow Cytometry

Apoptosis detection was performed using Annexin V-fluorescein isothiocyanate (FITC) apoptosis detection kit (BestBio, Shanghai, China). The transfected cells were detached with trypsin and washed with cold PBS. After that, the cells were resuspended in 1 × binding buffer at 1×10^5 cells/mL. Then, 5 μL FITC Annexin-V and 5 μL propidium iodide were appended to 100 μL cell suspension, and the sample was incubated without light exposure for 15 minutes, followed by supplement of 400 μL 1 × binding buffer. Cell apoptosis was analyzed by a flow cytometer (FACSCalibur, Becton-Dickinson) using CellQuest software (Becton Dickinson). Cell apoptosis is the sum of early apoptotic cells (quadrants Q1-4) and late apoptotic or necrotic cells (quadrants Q1-2).

Cell Transfection

miR-19b mimic/inhibitor and LV-CCL1 and corresponding controls were synthesized by GenePharma (Shanghai, China). All transfections were performed using Lipofectamine 2000 reagent (Invitrogen), and the transfection efficiency was examined by RT-qPCR.

Transwell Co-Culture System

H_2O_2-treated cells (1×10^5) were seeded into the basolateral chambers. For ADMSCs treatment, ADMSCs (5×10^5) were seeded into the apical chambers of 6-well cell culture inserts. For exosomes treatment, exosomes were appended to the culture medium at 2 μg of exosomes every 1×10^5 recipient cells. The 20 μM exosome inhibitor GW4869 (HY-19363, MedChemExpress, Monmouth Junction, NJ, USA) was supplemented to ADMSCs to restrict the production of exosomes.

Enzyme-Linked Immunosorbent Assay (ELISA)

The expression of apoptosis-related factors (C-caspase3: ab220655; Bcl-2: ab119506) and inflammation-related factors (IL-6: ab178013; IL-10: ab46034) in HaCaT cells were detected according to the instructions of ELISA kits (all from Abcam).

Wound Healing Assay

Cells were seeded into 6-well plates at 5×10^5 cells per well and cultivated for 12 hours. When reaching 80% confluence, the cells were induced with 300 μM H_2O_2 for 12 hours. After removing the medium, the wounds were created evenly with a sterile pipette tip. Each well was rinsed with PBS, and then supplemented with basic DMEM containing H_2O_2, ADMSCs, ADMSCs + GW4869, and exosome. The width between the 12nd hour and baseline was compared by Image-Pro Plus 6.0 software.

Exosome Internalization

Exosomes derived from ADMSCs were labeled with PKH26 (red, MINI26-1KT; Sigma-Aldrich). Fluorescence-labeled exosomes were co-cultured with different concentrations of H_2O_2-treated (0 μM, 100 μM, 200 μM, 300 μM) HaCaT cells and HSF in a 24-well plate for 48 hours. The nuclei were stained with Hoechst 33342 (HY-15559, MedChemExpress). The cells were captured under an inverted fluorescence microscope (NuoHaiLifeScience, Shanghai China).

Dual-Luciferase Reporter Gene Assay

The 293T cell line from the American Type Culture Collection (CRL-11268, ATCC, Manassas, VA, USA) was incubated with the medium in 24-well plates. The binding sites between miR-19b and CCL1 were predicted by Starbase (http://starbase.sysu.edu.cn/). cDNA fragment containing the predicted miR-19b binding site was amplified by PCR and then inserted into pGL3 vector for the generation of CCL1 wild-type (WT) vector. A QuikChange site-directed mutagenesis kit (Agilent, Roseville City, CA, USA) was utilized to obtain CCL1 mutant-type (MT) vector in the miR-19b binding sites. Next, the above-mentioned reporter vectors and transfection plasmids were co-transfected into 293T cells for 48 hours with the application of Lipofectamine 2000 (Invitrogen). The luciferase activity was assessed by a luciferase reporter assay system (Promega, Madison, WI, USA).

Radioimmunoprecipitation (RIP) Assay

The binding between miR-19b and CCL1 was detected using RIP kit (Millipore, Temecula, CA, USA). Cells were ice-bathed using an equal volume of RIP assay lysis buffer (Beyotime), and then centrifuged for 10 minutes at 14,000 rpm (4°C) to remove the supernatant. A part of the cell extract was used as input, while the rest was utilized for co-precipitation reaction with Ago2 antibody (ab32381, 1: 100; Abcam). IgG antibody (ab2410, 1: 100; Abcam) was utilized as a control. RNA was extracted from

the samples with TRIzol reagent (Invitrogen), and then the enrichment was analyzed by RT-qPCR.

Western Blot Assay

Cells were lysed with radioimmunoprecipitation assay lysis buffer (Beyotime) on ice for 30 minutes to obtain total protein. BCA kit was used for protein quantification (Thermo Fisher Scientific). The protein extract was applied to 10% sodium dodecyl sulfate-polyacrylamide gel electrophoresis and transferred onto a nitrocellulose membrane (Bio-Rad, Hercules, CA, USA). The membrane was probed with primary antibodies against TGF-β1 (1: 1000, #3709) and GAPDH (1: 1000, # 2118, loading control) (both from Cell Signaling Technology, Beverly, MA, USA) at 4°C overnight, and re-probed with secondary antibody, horseradish peroxidase (HRP)-conjectured goat anti-rabbit IgG H&L (1: 25000, ab205718, Abcam) for 1 hour at room temperature. The enhanced chemiluminescence system (Thermo Fisher Scientific) was implemented to detect band signals and then captured.

A Mouse Model of Skin Trauma

Fifteen Balb/C mice (20–25 g) were purchased from the Experimental Animal Center of the Third Affiliated Hospital of Zunyi Medical University. The dorsal region of the mice was shaved. A circular full-layer wound (1 cm in diameter) was created on the dorsal surface using a sterile pipette. The mice were classified into 3 groups, 5 in each group. The mice experienced subcutaneous injection of NC inhibitor- or miR-19b inhibitor-transfected ADMSCs-derived 100 μg exosomes (Exo-NC or Exo-inhibitor) dissolved in 100 μL PBS or an equal volume of PBS at tissues around wounds. The wound was disinfected with 0.5% iodine every day. The wound area was determined by drawing the wound edge on a transparent plastic film. The wound tissues and its surrounding area were harvested on the 8th day. The tissues were fixed in 10% paraformaldehyde and embedded in paraffin.

Hematoxylin-Eosin (HE) Staining

The obtained edge tissues of mouse wounds were fixed in 10% neutral formalin for at least 24 hours, dewaxed in xylene, dehydrated through a series of gradient ethanol, stained with hematoxylin and eosin solution and fixed in resin. The image was captured under an optical microscope.

Immunohistochemistry

The paraffin-embedded sections were dehydrated with a series of ethanol, washed with running water for 2 minutes, immersed in 3% H_2O_2 for 20 minutes, washed with distilled water for 2 minutes, and then rinsed with PBS for 3 minutes. The heat-mediated antigen retrieval was performed with Tris/ethylene diamine tetraacetic acid buffer (pH = 9.0). The samples were blocked by incubating in 10% normal goat serum for 20 minutes at room temperature. The slides were incubated with rabbit anti-mouse TGF-β1 primary antibody (1: 500, ab215715, Abcam) at 4°C overnight, and with goat anti-rabbit IgG H&L (1: 1000, ab6721, Abcam) and streptavidin working solution (0343–10000U; Imunbio, Beijing, China) at 37°C for 20 minutes. Subsequently, the sections were developed by diaminobenzidine (ST033; Whiga Biotech, Guangzhou, Guangdong, China), counterstained with hematoxylin (PT001; Bogoo Biotech, Shanghai, China), treated with 1% ammonia water, then dehydrated with gradient alcohol, cleared with xylene, and fixed with neutral resin. The sections were captured and viewed under an optical microscope.

Statistical Analysis

All quantitative data were the mean ± standard deviation of at least three independent experiments, and processed by SPSS 22.0 statistical software (IBM, Armonk, NY, USA). The comparison between the two groups was carried out by unpaired *t*-test, while the comparison for multiple groups was analyzed by one-way or two-way analysis of variance (ANOVA), followed by Tukey's post hoc test. $p < 0.05$ indicated statistical significance.

Results

Identification of ADMSCs and ADMSCs-Derived Exosomes

The protein expression on the surface markers of ADMSCs was analyzed by flow cytometry. It was found that ADMSCs were found to be positive for MSC surface markers of (CD44 and CD105), and were found to be negative for hematopoietic stem cell markers (CD34 and CD45) (Figure 1A). After osteogenic culture of ADMSCs for three weeks, calcium precipitation was observed with alizarin red staining (Figure 1B), suggesting that ADMSCs had the osteogenic differentiation ability. After adipogenic culture of ADMSCs for two weeks, fat droplets were seen in cells with oil red O staining (Figure 1C), indicating that

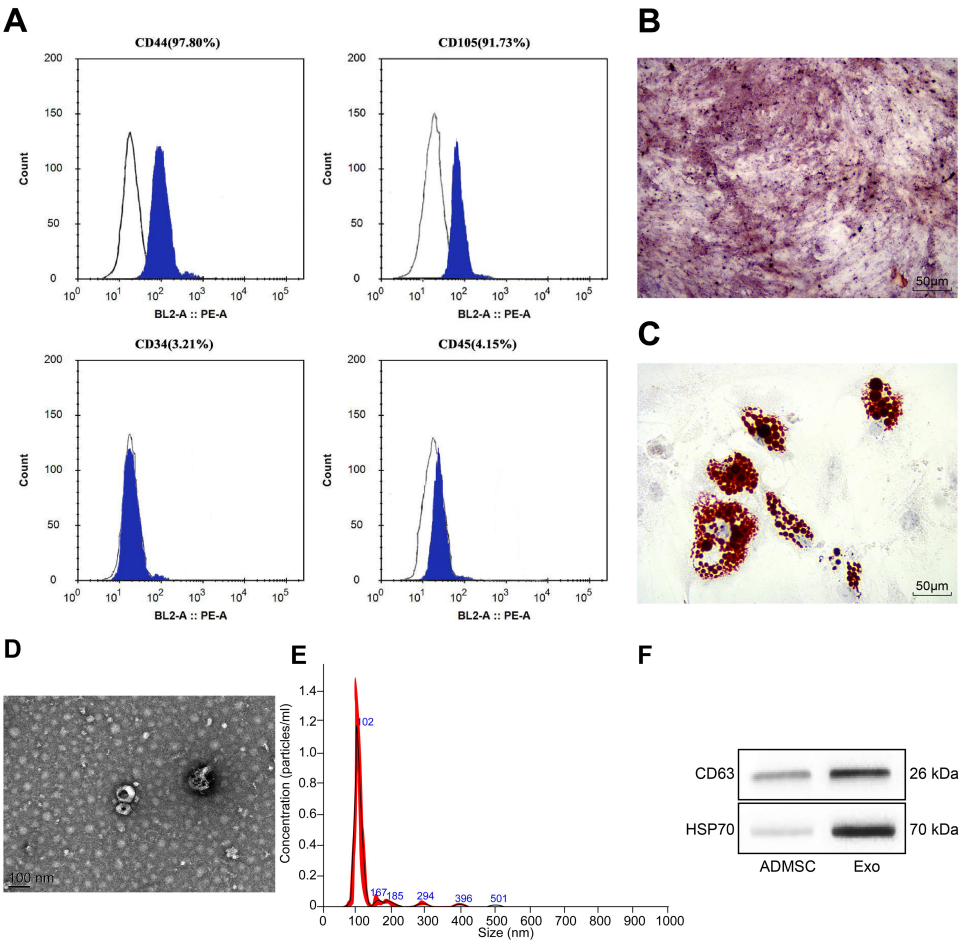

Figure 1 Identification of ADMSCs and their derived exosomes. (**A**) The surface antigen of cells was detected by flow cytometry. (**B**) Alizarin red staining was used to detect the osteogenic differentiation ability of ADMSCs. (**C**) Oil Red O staining was used to detect the adipogenic differentiation ability of ADMSCs. (**D**) The structure of exosomes was observed by a TEM. (**E**) The size of exosomes was analyzed by NTA. (**F**) The exosome marker proteins were detected by Western blot analysis.

ADMSCs had the adipogenic differentiation ability. This indicates that the purchased cells are ADMSCs.

Exosomes extracted from ADMSCs were observed by a TEM, and oval-shaped membrane vesicles were observed (Figure 1D). The results of NTA suggested that the exosome size was about 100 nm (Figure 1E). Western blot assay showed that exosomes expressed specific marker proteins CD63 and HSP70 (Figure 1F). It suggests that we have successfully extracted the exosomes of ADMSCs.

ADMSCs and Their Derived Exosomes Have a Therapeutic Effect on H_2O_2 -Treated HaCaT Cells

HaCaT cells were induced with varying concentrations of H_2O_2. Based on results of MTT assay, we found that the viability of HaCaT cells decreased in a concentration-dependent manner (Figure 2A). Meanwhile, flow cytometry results indicated that the apoptosis rate of cells increased in a concentration-dependent manner (Figure 2B). This indicates that we have successfully developed a cell model of skin damage. When the concentration of H_2O_2 reached 300 μM, the cells already showed lower viability and higher apoptosis rate, so we chose 300 μM H_2O_2-treated HaCaT cells for subsequent experiments (the Model group).

To investigate whether ADMSCs had a therapeutic effect on H_2O_2-treated HaCaT cells, we designed the Tanswell co-culture system (Figure 2C). According to findings of MTT assay and flow cytometry, we found that ADMSCs and exosome treatment both significantly improved cell viability and suppressed cell apoptosis, while the therapeutic ability of ADMSCs was significantly suppressed upon treatment of exosome inhibitor GW4869 (Figure 2D and E). Next, the expression of apoptosis-related proteins C-caspase3 and Bcl-2 and inflammation-related factors IL-6 and IL-10 were detected using ELISA kits, and the obtained results indicated that ADMSCs and exosome treatment reduced expression of C-caspase3 and IL-6 and elevated expression of Bcl-2 and

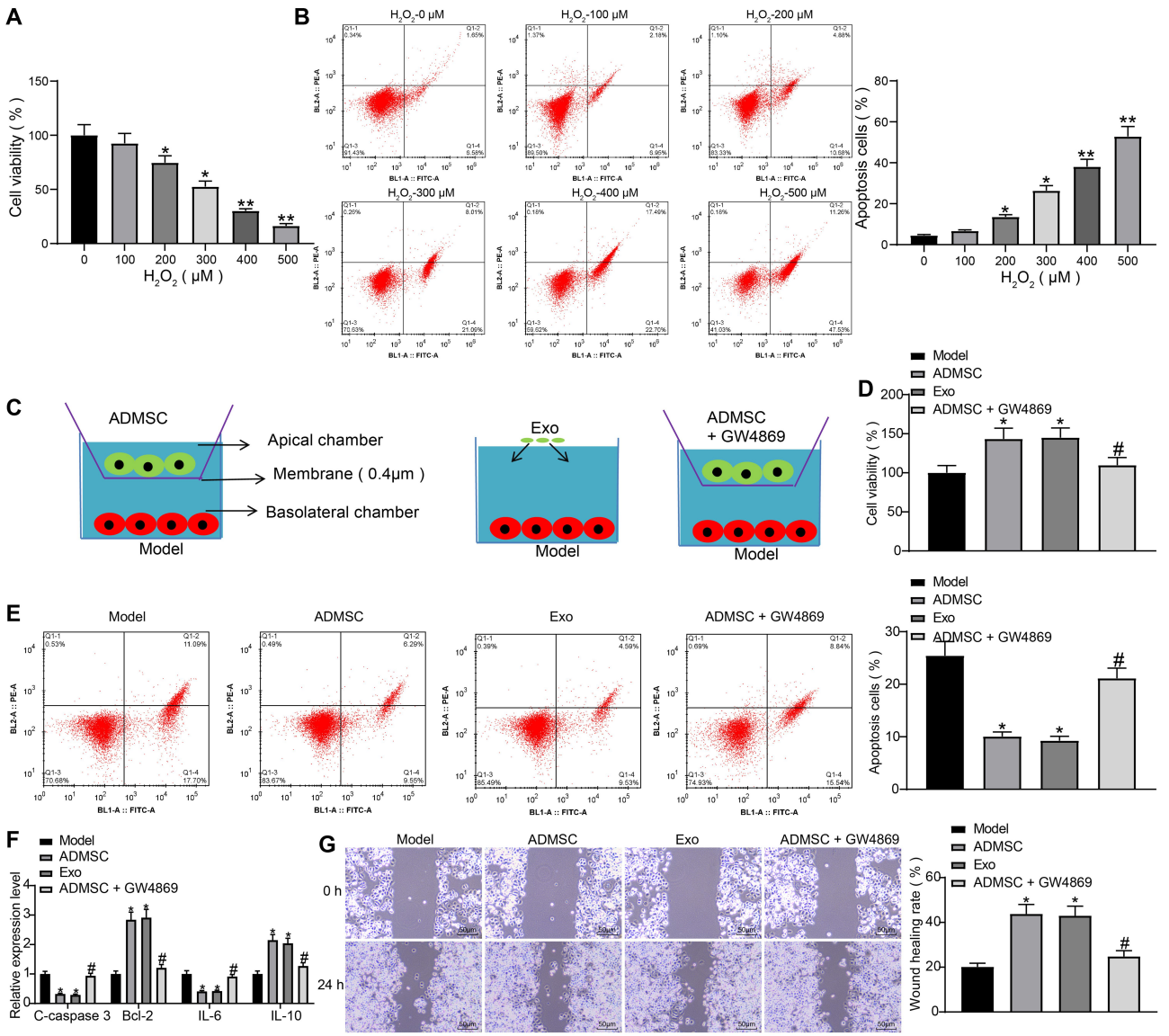

Figure 2 ADMSCs and their derived exosomes alleviate H_2O_2-induced HaCaT cell damage. (**A**) MTT assay was used to measure the effect of different concentrations of H_2O_2 on the viability of HaCaT cells (one-way ANOVA, *P < 0.05 or **P < 0.01 vs 0 μM). (**B**) Flow cytometry was implemented to measure the effect of different concentrations of H_2O_2 on the apoptosis of HaCaT cells (one-way ANOVA, *P < 0.05 or **P < 0.01 vs 0 μM). (**C**) Transwell co-culture system. (**D**) MTT assay was utilized to measure the effect of ADMSCs and exosome treatment on the viability of HaCaT cells treated with H_2O_2 (one-way ANOVA, *P < 0.05 vs the model group; # P < 0.05 vs ADMSCs group). (**E**) Flow cytometry was performed to measure the effect of ADMSCs and exosome treatment on the apoptosis of HaCaT cells treated with H_2O_2 (one-way ANOVA, *P < 0.05 vs the model group; # P < 0.05 vs ADMSCs group). (**F**) ELISA was utilized to measure the effect of ADMSCs and exosome treatment on the expression of apoptosis-related genes (C-caspase3, Bcl-2) and inflammation-related genes (IL-6, IL-10) in HaCaT cells treated with H_2O_2 (one-way ANOVA, *P < 0.05 vs the model group; # P < 0.05 vs ADMSCs group). (**G**) Wound healing test was performed to measure the effect of ADMSCs and exosome treatment on the migration ability of HaCaT cells treated with H_2O_2 (one-way ANOVA, *P < 0.05 vs the model group; # P < 0.05 vs ADMSCs group).

IL-10, while the treatment of GW4869 exhibited an inverse tendency (Figure 2F). The wound healing test revealed that ADMSCs and exosome treatment promoted HaCaT cell migration, while GW4869 inhibited the promoted pro-migratory effect of ADMSCs on HaCaT cells (Figure 2G). To conclude, ADMSCs have a therapeutic effect on H_2O_2-treated HaCaT cells, and this effect mainly depends on the derived exosomes.

H_2O_2 Treatment Promotes the Internalization of Exosomes

To verify whether exosomes could act on HaCaT cells, the exosomes secreted by ADMSCs were labeled with PKH26. HaCaT cells exposed to different concentrations of H_2O_2 were treated with the same concentrations of labeled exosomes. After 48 hours, the concentrations of exosomes taken up by the cells were observed. We found

that after 48 hours, HaCaT obviously phagocytosed exosomes, and the intake of exosomes increased with increasing H_2O_2 concentration (Figure 3). This indicates that the cell damage caused by H_2O_2 promoted HaCaT cell phagocytosing of exosomes, thereby reducing cell damage.

Exosomal miR-19b is Effective in Ameliorating H_2O_2-Treated HaCaT Cells

As previously reported, miR-19b reduced extracellular matrix degradation and inflammatory damage,[15] while inhibiting inflammation and reducing extracellular matrix degradation can promote wound healing.[23] miR-19b expression was measured by RT-qPCR in HaCaT cells treated with varying concentrations of H_2O_2, and it was found that miR-19b expression decreased as the concentration of H_2O_2 increased (Figure 4A). Additionally, miR-19b expression in the supernatant after centrifugation and exosomes was detected by RT-qPCR, and it was indicated that miR-19b was significantly enriched in exosomes (Figure 4B). Meanwhile, miR-19b expression in HaCaT cells under the Transwell co-culture system was measured, and results suggested that ADMSCs and exosome treatment increased the expression of miR-19b, while GW4869 reduced miR-19b expression (Figure 4C). This indicated that ADMSCs shuttled miR-19b by secreting exosomes, thereby increasing miR-19b expression in the recipient cells.

miR-19b inhibitor and its control were transfected into ADMSCs, and the obtained exosomes were collected and named as Exo-NC or Exo-inhibitor, respectively. miR-19b expression in two groups of exosomes was measured by RT-qPCR, and it was suggested that miR-19b inhibitor reduced the expression of miR-19b in exosomes produced by ADMSCs (Figure 4D). Next, Exo-NC and Exo-inhibitor were co-cultured with H_2O_2-treated HaCaT cells. The corresponding findings demonstrated that Exo-inhibitor reduced cell viability, elevated apoptosis rate, increased expression of C-caspase3 and IL-6, decreased expression of Bcl-2 and IL-10, as well as suppressed migration rate (Figure 4E–H). These data indicate that exosomes mainly exert effects through miR-19b. Inhibition of miR-19b could reduce the therapeutic effect of exosomes.

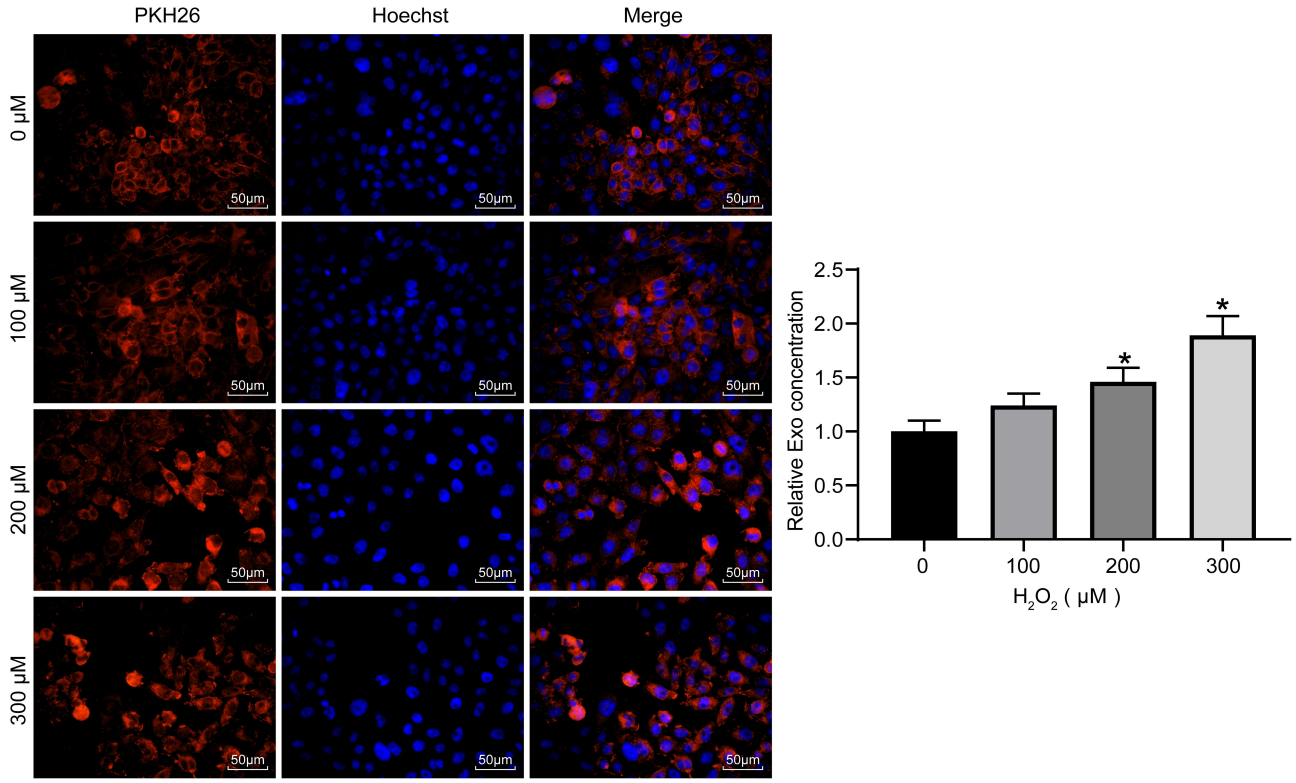

Figure 3 Internalization of exosomes. Exosomes labeled with the same amount of PKH26 were co-cultured with HaCaT treated with different concentrations of H_2O_2 to measure the exosome uptake of cells (one-way ANOVA, *$P < 0.05$ vs 0 μM).

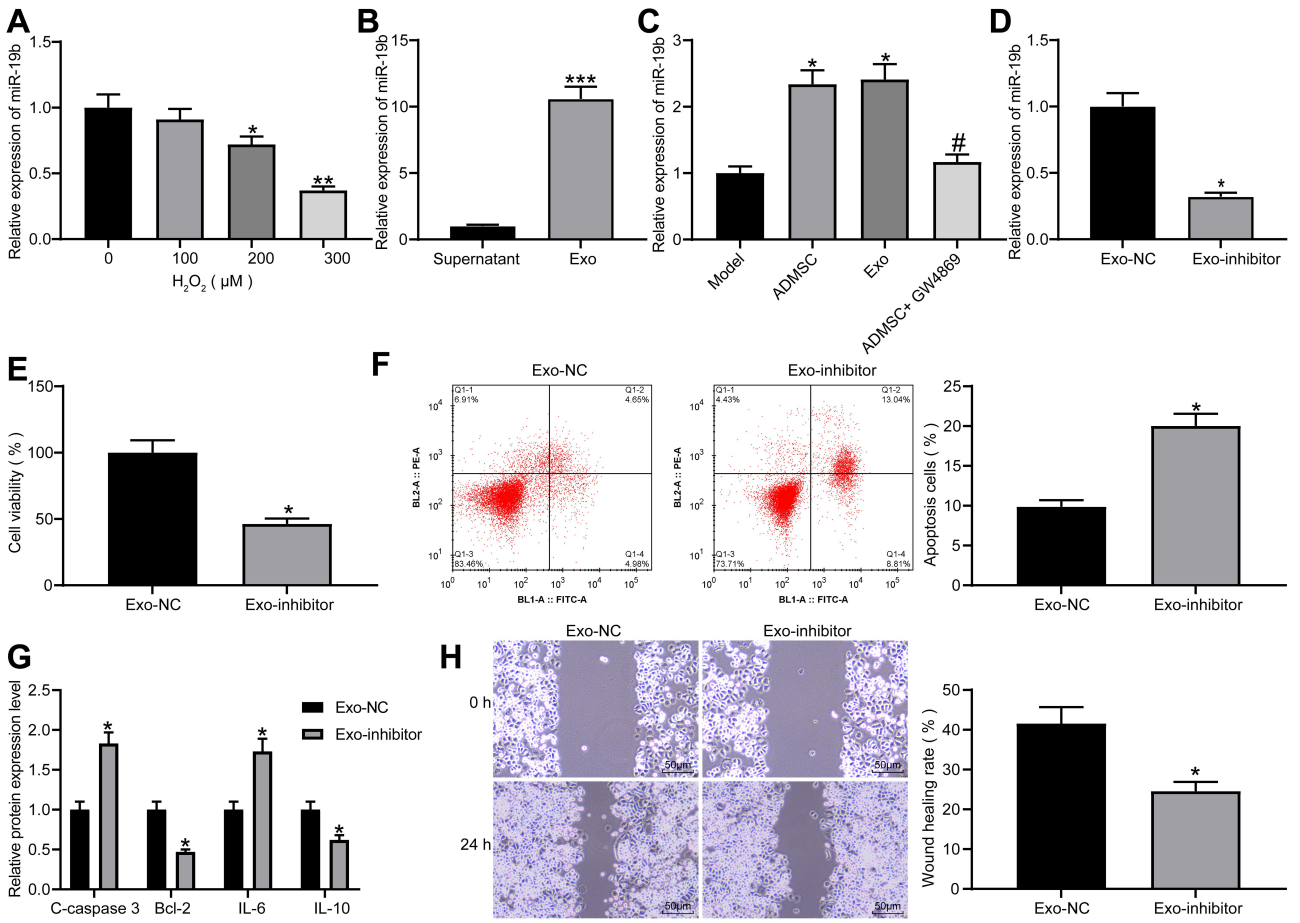

Figure 4 Exosomal miR-19b alleviates H_2O_2-induced HaCaT cell damage. (**A**) RT-qPCR was conducted to determine miR-19b expression in HaCaT cells treated with different concentrations of H_2O_2 (one-way ANOVA, $^*P < 0.05$ or $^{**}P < 0.01$ vs 0 μM). (**B**) RT-qPCR was carried out to detect miR-19b expression in supernatant and exosomes (unpaired *t* test, $^{***}P < 0.001$). (**C**) RT-qPCR was performed to detect miR-19b expression in Transwell co-culture system (one-way ANOVA, $^*P < 0.05$ vs the model group; # $P < 0.05$ vs ADMSCs group). (**D**) RT-qPCR was conducted to determine miR-19b expression in ADMSCs-derived exosomes that had been transfected with miR-19b inhibitor (unpaired *t* test, $^*P < 0.05$). (**E**) MTT assay was used to measure the viability of H_2O_2-treated HaCaT cells that had been co-cultured with Exo-NC and Exo-inhibitor (unpaired *t* test, $^*P < 0.05$). (**F**) Flow cytometry was implemented to measure the apoptosis of H_2O_2-treated HaCaT cells that had been co-cultured with Exo-NC and Exo-inhibitor (unpaired *t* test, $^*P < 0.05$). (**G**) ELISA was utilized to measure the expression of apoptosis-related proteins (C-caspase3, Bcl-2) and inflammation-related proteins (IL-6, IL-10) in H_2O_2-treated HaCaT cells that had been co-cultured with Exo-NC and Exo-inhibitor (unpaired *t* test, $^*P < 0.05$). (**H**) Wound healing was performed to measure the migration ability of H_2O_2-treated HaCaT cells that had been co-cultured with Exo-NC and Exo-inhibitor (unpaired *t* test, $^*P < 0.05$).

miR-19b Targets CCL1 to Regulate the TGF-β Signaling Pathway

The online website StarBase (http://starbase.sysu.edu.cn/) predicted that miR-19b targeted CCL1 (Figure 5A). CCL1 is a typical inflammatory factor and its expression is not conducive to wound healing.[19] In HaCaT cells treated with varying concentrations of H_2O_2, CCL1 expression was tested by RT-qPCR and found to increase in a concentration-dependent manner (Figure 5B). MiR-19b mimic was transfected into H_2O_2-treated cells. The determination of miR-19b expression by RT-qPCR confirmed the effective transfection (Figure 5C). Through luciferase activity assay, we found that miR-19b mimic declined the luciferase activity of WT-CCL1, but had no impact on the MT form (Figure 5D). Their binding relationship was further verified by RIP assay, the obtained findings indicated that anti-AGO2 significantly enriched miR-19b and CCL1 (Figure 5E). These evidences suggest that miR-19b targets CCL1.

The activation of TGF-β pathway is thought to promote wound healing.[24,25] CCL1 expression in H_2O_2-treated HaCaT cells that had been introduced with miR-19b mimic, miR-19b mimic + LV-CCL1 or its control was determined by RT-qPCR. The suppressive effect of miR-19b mimic on CCL1 expression was reversed by LV-CCL1 (Figure 5F). Further Western blot assay revealed that miR-19b mimic promoted

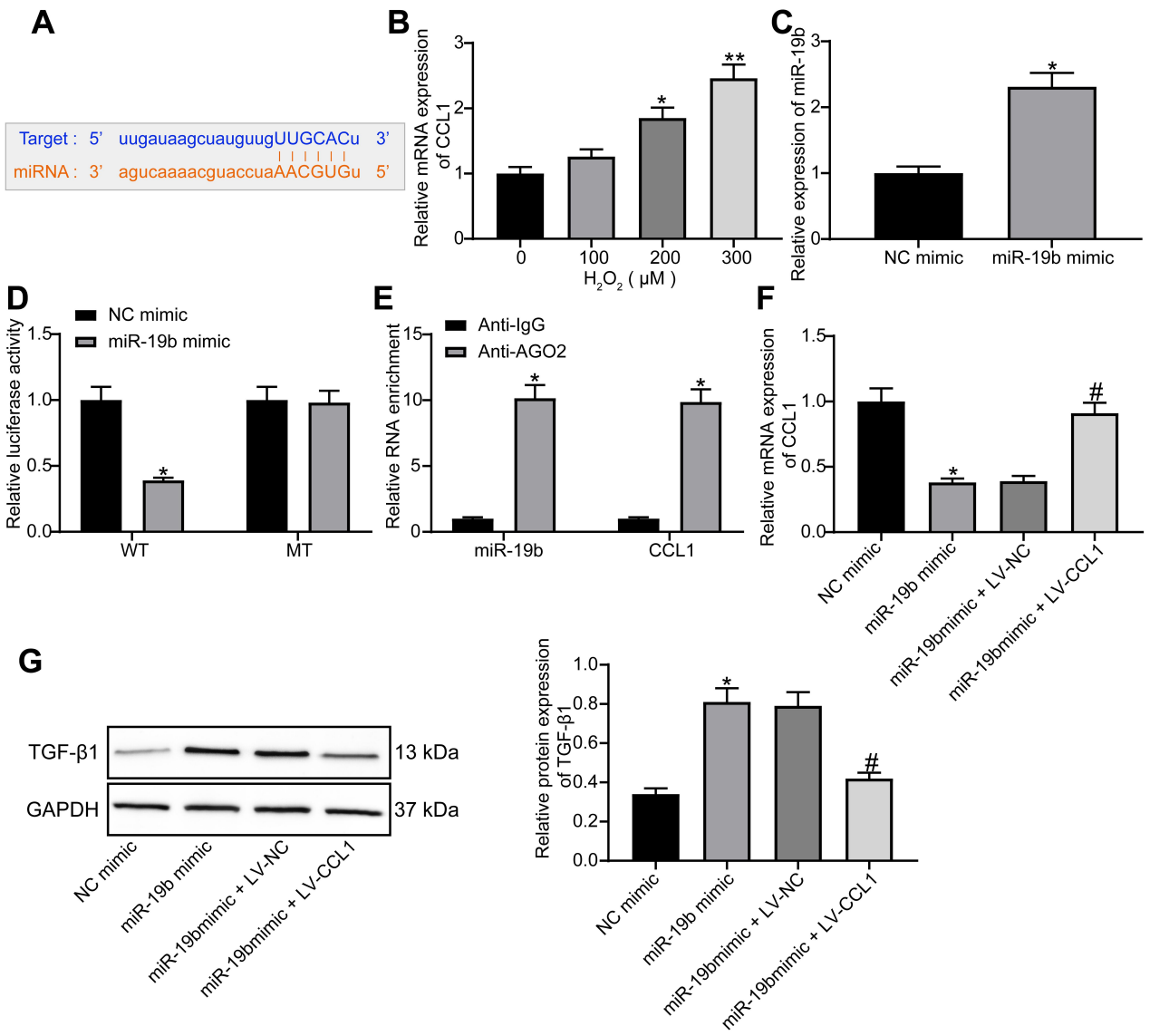

Figure 5 miR-19b regulates the TGF-β pathway by targeting CCL1. (**A**) Potential binding sites between miR-19b and CCL1. (**B**) RT-qPCR was conducted to determine CCL1 expression in HaCaT cells treated with different concentrations of H_2O_2 (one-way ANOVA, $^*P < 0.05$ or $^{**}P < 0.01$ vs 0 μM). (**C**) RT-qPCR was carried out to measure the transfection efficiency of miR-19b mimic (unpaired *t* test, $^*P < 0.05$). (**D**) Dual-luciferase reporter gene assay was performed to evaluate the effect of miR-19b mimic on the luciferase activity of WT-CCL1 or MT-CCL1 (two-way ANOVA, $^*P < 0.05$). (**E**) RIP assay was used to measure the enrichment of miR-19b and CCL1 (two-way ANOVA, $^*P < 0.05$). (**F**) RT-qPCR was implemented to measure the effect of miR-19b mimic and LV-CCL1 on CCL1 expression (one-way ANOVA, $^*P < 0.05$ vs the NC mimic group; $^{\#}P < 0.05$ vs the miR-19b mimic + LV-NC group). (**G**) Western blot assay was implemented to measure the effect of miR-19b mimic and LV-CCL1 on TGF-β pathway (one-way ANOVA, $^*P < 0.05$ vs the NC mimic group; $^{\#}P < 0.05$ vs the miR-19b mimic + LV-NC group).

TGF-β1 expression, and this promotion was partially reversed by LV-CCL1 (Figure 5G). To conclude, miR-19b regulates the TGF-β pathway by targeting CCL1.

Exosomal miR-19b Contributes to the Proliferation and Migration of HSF

We have demonstrated the effect of exosomal miR-19b on HaCaT cells and their mechanism of action. Moreover, HSF also played an important role in wound healing.[26,27] We therefore experimentally tested whether exosomal miR-19b could have an effect on HSF.

We first confirmed that exosomes could be taken up by HSF, and we observed a significant uptake of exosomes by HSF after 48 hours of incubation with exosomes (Figure 6A). HSF were treated with 300 μM H_2O_2 (the control group was treated with PBS). A proportion of H_2O_2-treated HSF were further co-cultured with Exo-NC or Exo-inhibitor, respectively. The expression of miR-19b in each group of cells was detected by RT-qPCR (Figure 6B). We

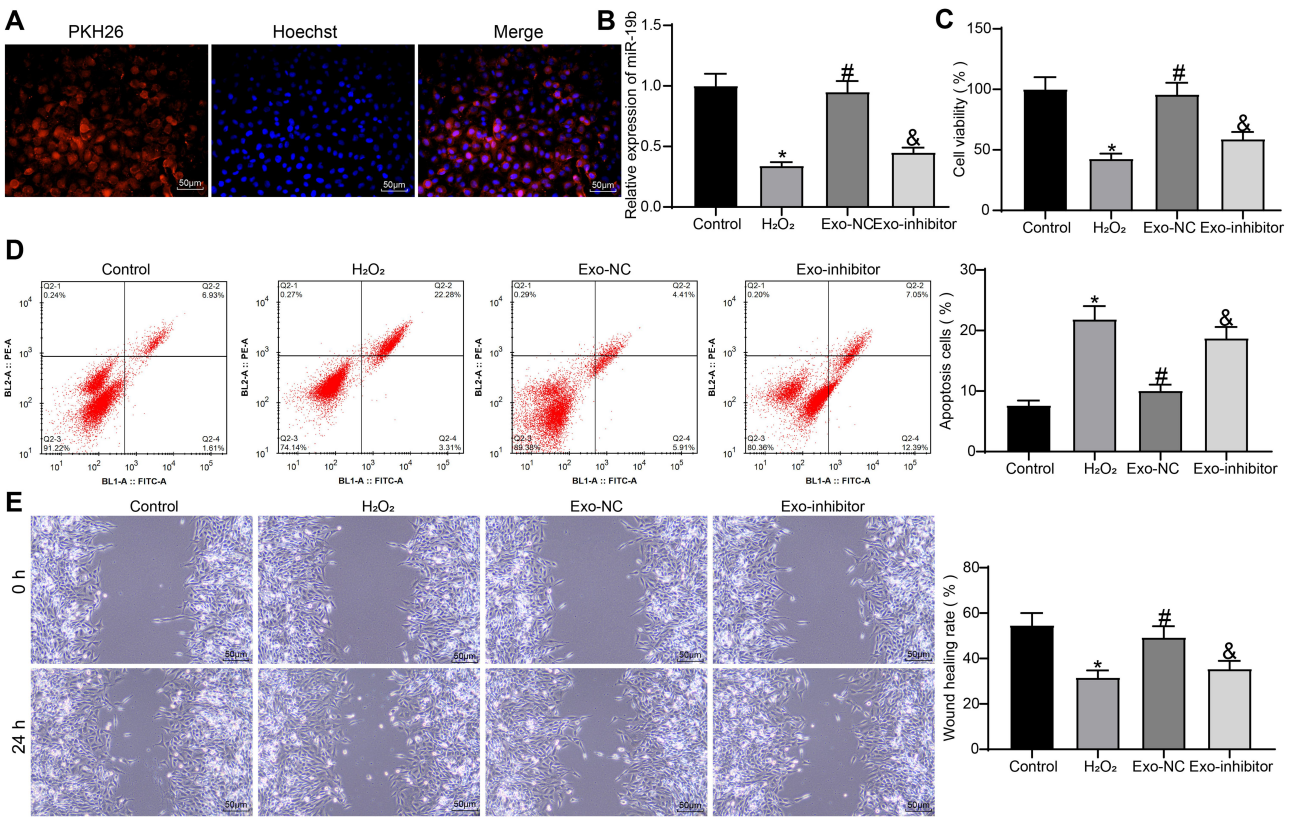

Figure 6 Exosomal miR-19b promotes HSF growth and migration. (**A**) HSF uptake of exosomes. (**B**) Expression of miR-19b in HSF cells was detected by RT-qPCR (one-way ANOVA, **P* < 0.05 vs the Control group; #*P* < 0.05 vs the H_2O_2 group; &*P* < 0.05 vs the Exo-NC group). (**C**) MTT assay to detect the viability of cells (one-way ANOVA, **P* < 0.05 vs the Control group; #*P* < 0.05 vs the H_2O_2 group; &*P* < 0.05 vs the Exo-NC group). (**D**) Flow cytometry to detect apoptosis rate of cells (one-way ANOVA, **P* < 0.05 vs the Control group; #*P* < 0.05 vs the H_2O_2 group; &*P* < 0.05 vs the Exo-NC group). (**E**) Wound healing detected the migration ability of HSF cells in each group (one-way ANOVA, **P* < 0.05 vs the Control group; #*P* < 0.05 vs the H_2O_2 group; &*P* < 0.05 vs the Exo-NC group).

found that H_2O_2 treatment led to a decrease in miR-19b expression in HSF, and exosome treatment led to an increase in miR-19b expression to varying degrees. Among them, the Exo-inhibitor-treated HSF showed a significant decrease in miR-19b expression compared to the Exo-NC-treated HSF. Cell viability was measured by MTT (Figure 6C). We observed that H_2O_2 treatment led to a reduction in cell viability, and that H_2O_2-induced reduction in cell viability could be rescued by exosome treatment, with Exo-NC having a significantly higher rescue effect on cell viability than Exo-inhibitor. Flow cytometry was used to identify the rate of apoptosis (Figure 6D). H_2O_2 treatment resulted in an increased rate of HSF apoptosis, and exosome treatment inhibited H_2O_2-induced HSF apoptosis to varying degrees. The inhibitory effect of Exo-inhibitor on apoptosis was significantly attenuated compared to Exo-NC. Finally, wound healing assay showed that H_2O_2 inhibited cell migration, while Exo-NC promoted cell migration ability significantly relative to Exo-inhibitor (Figure 6E).

ADMSC-Derived Exosomes Promote the Wound Healing of Skin-Injured Mice Through miR-19b

Furthermore, Exo-inhibitor, Exo-NC and PBS were injected around the wounds of skin-injured mice. We found that the wound tissues of mice gradually healed over time, and meanwhile, the two groups of mice treated with exosomes exhibited accelerated wound healing to varying degrees, and Exo-inhibitor was less effective than Exo-NC (Figure 7A). Eight days later, the tissues around the wounds were harvested. The wound tissues observed by HE staining suggested that the exosome-treated mice had less inflammatory infiltration around the wound and had thick granulation tissues. Exo-NC group mice had the least pathological degree (Figure 7B). The expression of miR-19b and CCL1 in tissues were detected by RT-qPCR, and it was suggested that exosome treatment increased miR-19b expression and decreased CCL1 expression to different degrees, among which the function of Exo-NC was more obvious (Figure 7C). Immunohistochemistry for the detection of TGF-β pathway revealed that exosome treatment

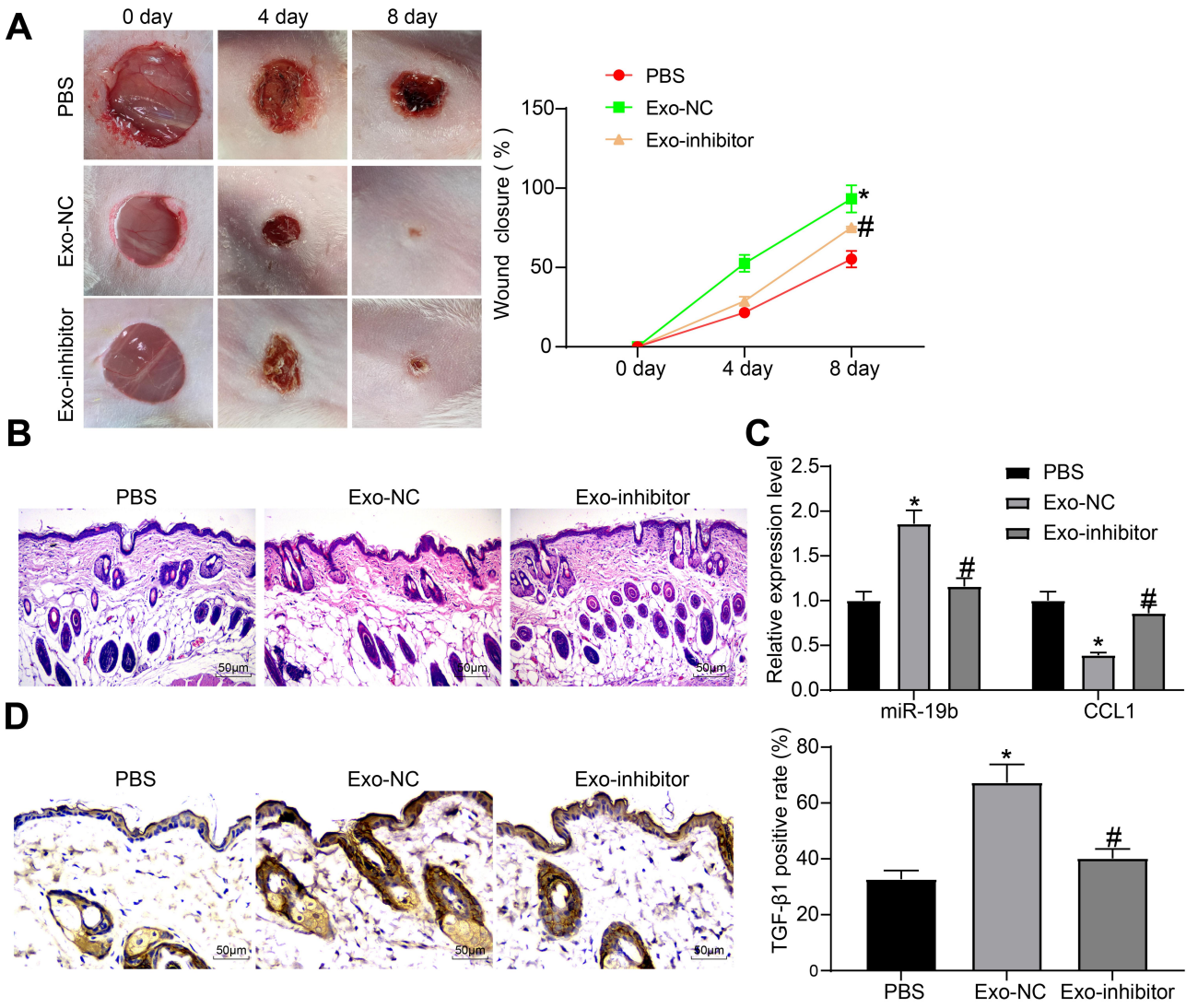

Figure 7 Exosome promotes wound healing in mice. (**A**) Wound healing state of mice treated with PBS, Exo-NC or Exo-inhibitor, respectively (two-way ANOVA, **P* < 0.05 vs the PBS group; #*P* < 0.05 vs the Exo-NC group). (**B**) HE staining was used to observe the pathological conditions of the tissues around the mouse wound. (**C**) RT-qPCR was implemented to measure the expression of miR-19b and CCL1 (two-way ANOVA, **P* < 0.05 vs the PBS group; #*P* < 0.05 vs the Exo-NC group). (**D**) Immunohistochemistry was performed to measure the expression of TGF-β1 in the tissues around the mouse wound (one-way ANOVA, **P* < 0.05 vs the PBS group; #*P* < 0.05 vs the Exo-NC group).

increased TGF-β1 expression to varying degrees, while the positive rate in the Exo-NC group was the highest (Figure 7D).

Discussion

Skin is a complex organ of the dermis, epidermis and skin appendages, while wound healing in adult mammals results in scarring without skin appendages.[28] It has been presented that miRs could modulate gene expression post-transcriptionally through the binding to the 3′untranslated regions of target mRNAs.[29] Some studies have reported that miRs are participated in skin wound healing with a promotive role,[14,30] while the role of miR-19b in skin wound healing has not been discussed. In a study conducted by Suga et al, it is shown that serum CCL1 level is related to pruritus in patients with cutaneous T-cell lymphoma.[31] Interestingly, CCL1 was observed to possibly contribute to chemoresistance in colorectal cancer cells via TGF-β.[32] The current study was designed to probe into the impact of ADMSCs-derived exosomal miR-19b on skin wound healing process via modulating CCL1 and the TGF-β pathway.

Our results demonstrated that exosomes treatment enhanced miR-19b expression and lowered CCL1 expression in HaCaT cells. A recent study has presented that miR-19b-3p level is markedly reduced in the serum from sepsis patients in relation to healthy controls.[33] Another study has presented that

miR-19b expression is aberrantly diminished in the murine allergic conjunctivitis model,[34] but the expression of miR-19b in skin injury-related cells has not been reported. It is established that CCL1 mRNA and protein expression is dramatically enhanced in the acute lesional skin of atopic dermatitis patients relative to that in their non-lesional skin or in the lesional skin of psoriasis patients,[20] which was in accord with our findings. Another study also purports that MSCs reduce the expression of chemokines such as CCL1 in the skin.[35] In addition, our study reported that miR-19b targeted CCL1 in HaCaT cells. A study has demonstrated that miR-20a-5p targets to CCL1 in patients with Vogt-Koyanagi-Harada disease.[36] The interactions between exosomes and miR-19b as well as the targeting relationships between CCL1 and miR-19b need further exploration.

A main result emerging from our data was that ADMSCs-derived exosomes alleviated cell injury, inhibited apoptosis and enhanced vitality of HaCaT cells and HSF. It has been reported that that ADMSC-derived exosomes elevate cell proliferation and migration as well as prevent cell apoptosis in cutaneous wound healing.[22,37] It has also been suggested previously that ADMSC-exosomes facilitate cell proliferation and migration as well as suppress cell apoptosis of HaCaT and HDF cells impaired by H_2O_2.[21] Another main result from our data was that inhibition of miR-19b in ADMSCs by miR-19b inhibitor at least partially abrogated the role of exosomes in accelerating recovery from cell injury in HaCaT cells and HSF. A study has verified that overexpressed miR-19b in the extracellular vesicles derived from differentiated PC12 cells and MSCs inhibits the apoptosis of neuron cells.[38] It is displayed that restoration of miR-19b markedly mitigates the endothelial cells apoptosis.[39] Meanwhile, up-regulating miR-19b accelerates proliferation and differentiation while suppresses apoptosis in P19 cells in cardiac differentiation in vitro.[40] Restoring miR-19b reduces cell apoptosis and expedites the viability as well as increased Bcl-2/Bax ratios in H/R-induced PC12 and BV2 cells.[41] Except that, our study also indicated that inhibition of miR-19b in exosomes increased levels of IL-6 and decreased levels of IL-10. Li et al have supported that transfection of miR-19 inhibitor promotes release of cytokines IL-6 in fibroblast-like synoviocytes.[42] Another article has demonstrated that miR-19a results in the inhibition of IL-10 in peripheral dendritic cells, which is important in the nasal polyp immune therapy.[43] In a word, exosomes and overexpressed miR-19b have a good effect in skin wound healing although the role of miR-19b needs further exploration.

Furthermore, this study suggested that miR-19b mimic significantly promoted the expression of TGF-β1, and this promotion was partially reversed by LV-CCL1. It is previously reported that in human immortalized keratinocyte cells, NRF2 contributes to wound healing by increasing proliferation and migration, decreasing apoptosis, and increasing the expression of TGF-β1.[24] Xiao et al have found that ozone oil treatment could activate fibroblasts by upregulating TGF-β1 in fibroblasts.[25] These data imply that activation of TGF-β pathway is thought to promote wound healing. Nevertheless, the

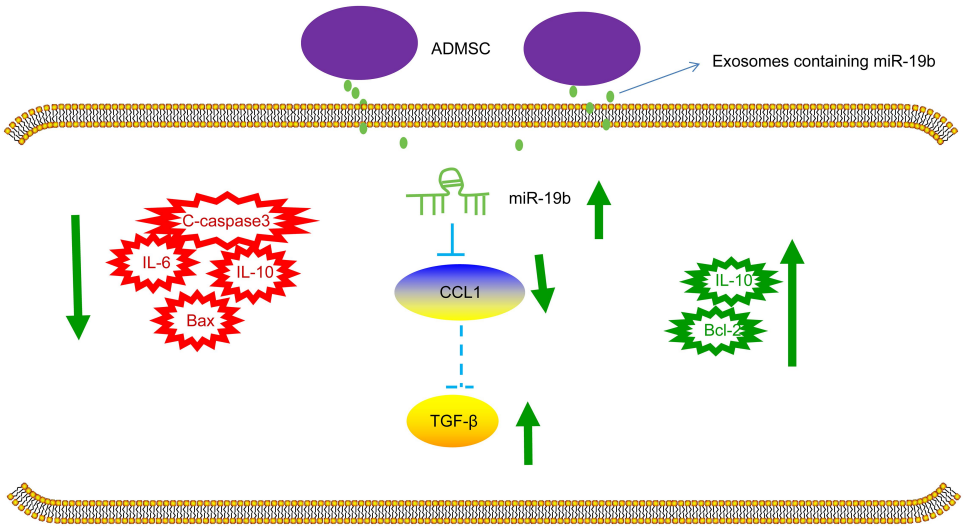

Figure 8 The mechanistic diagram indicates that ADMSCs-derived exosomal miR-19b promotes the activation of TGF-β signaling pathway by targeting CCL1, which inhibits the occurrence of inflammation and reduces the apoptosis of cells, thereby promoting the healing of skin wounds.

relation between miR-19b and TGF-β1 needs further confirmation.

To briefly conclude, our study suggests that ADMSCs-derived exosomal miR-19b promotes skin wound healing via targeting CCL1 and regulating TGF-β pathway (Figure 8). These findings provide a novel insight in a target therapy for skin wound healing. However, a conclusion concerning the effects of ADMSCs-derived exosomal miR-19b in skin wound healing cannot be made clearly due to limited known researches on this, which should be confirmed in the future clinical trials.

Disclosure

The authors declare there is no conflicts of interest in this work.

References

1. Zhao Y, Wang Q, Jin Y, et al. Discovery and Characterization of a High-Affinity Small Peptide Ligand, H1, Targeting FGFR2IIIc for Skin Wound Healing. *Cell Physiol Biochem*. 2018;49(3):1033–1048. doi:10.1159/000493287
2. Chanda A, Unnikrishnan V, Flynn Z, Lackey K. Experimental study on tissue phantoms to understand the effect of injury and suturing on human skin mechanical properties. *Proc Inst Mech Eng H*. 2017;231(1):80–91. doi:10.1177/0954411916679438
3. Valvis SM, Waithman J, Wood FM, Fear MW, Fear VS. The Immune Response to Skin Trauma Is Dependent on the Etiology of Injury in a Mouse Model of Burn and Excision. *J Invest Dermatol*. 2015;135(8):2119–2128. doi:10.1038/jid.2015.123
4. Arias JI, Parra N, Beato C, et al. Different Trypanosoma cruzi calreticulin domains mediate migration and proliferation of fibroblasts in vitro and skin wound healing in vivo. *Arch Dermatol Res*. 2018;310(8):639–650. doi:10.1007/s00403-018-1851-7
5. Roh J-L, Lee J, Kim EH, Shin D. Plasticity of oral mucosal cell sheets for accelerated and scarless skin wound healing. *Oral Oncol*. 2017;75:81–88. doi:10.1016/j.oraloncology.2017.10.024
6. Yang F, Qin X, Zhang T, Lin H, Zhang C. Evaluation of Small Molecular Polypeptides from the Mantle of Pinctada Martensii on Promoting Skin Wound Healing in Mice. *Molecules*. 2019;24(23):23. doi:10.3390/molecules24234231
7. Li Q, Zhao H, Chen W, Huang P, Bi J. Human keratinocyte-derived microvesicle miRNA-21 promotes skin wound healing in diabetic rats through facilitating fibroblast function and angiogenesis. *Int J Biochem Cell Biol*. 2019;114:105570. doi:10.1016/j.biocel.2019.105570
8. Sanchez-Sanchez R, Brena-Molina A, Martinez-Lopez V, et al. Generation of Two Biological Wound Dressings as a Potential Delivery System of Human Adipose-Derived Mesenchymal Stem Cells. *ASAIO J*. 2015;61(6):718–725. doi:10.1097/MAT.0000000000000277
9. Chicharro D, Carrillo JM, Rubio M, et al. Combined plasma rich in growth factors and adipose-derived mesenchymal stem cells promotes the cutaneous wound healing in rabbits. *BMC Vet Res*. 2018;14(1):288. doi:10.1186/s12917-018-1577-y
10. Qiu H, Liu S, Wu K, Zhao R, Cao L, Wang H. Prospective application of exosomes derived from adipose-derived stem cells in skin wound healing: A review. *J Cosmet Dermatol*. 2020;19(3):574–581. doi:10.1111/jocd.13215
11. Ding J, Wang X, Chen B, Zhang J, Xu J. Exosomes Derived from Human Bone Marrow Mesenchymal Stem Cells Stimulated by Deferoxamine Accelerate Cutaneous Wound Healing by Promoting Angiogenesis. *Biomed Res Int*. 2019;2019:9742765. doi:10.1155/2019/9742765
12. Cho BS, Kim JO, Ha DH, Yi YW. Exosomes derived from human adipose tissue-derived mesenchymal stem cells alleviate atopic dermatitis. *Stem Cell Res Ther*. 2018;9(1):187. doi:10.1186/s13287-018-0939-5
13. Li M, Cui X, Guan H. MicroRNAs: pivotal regulators in acute myeloid leukemia. *Ann Hematol*. 2020;99(3):399–412. doi:10.1007/s00277-019-03887-5
14. Long S, Zhao N, Ge L, et al. MiR-21 ameliorates age-associated skin wound healing defects in mice. *J Gene Med*. 2018;20(6):e3022. doi:10.1002/jgm.3022
15. Duan L, Duan D, Wei W, et al. MiR-19b-3p attenuates IL-1β induced extracellular matrix degradation and inflammatory injury in chondrocytes by targeting GRK6. *Mol Cell Biochem*. 2019;459(1–2):205–-214. doi:10.1007/s11010-019-03563-2
16. Li D, Peng H, Qu L, et al. miR-19a/b and miR-20a promote wound healing by regulating the inflammatory response of keratinocytes. *J Invest Dermatol*. 2020. doi:10.1016/j.jid.2020.06.037
17. Wang Z-W, Zhu X. Exosomal miR-19b-3p communicates tubular epithelial cells and M1 macrophage. *Cell Death Dis*. 2019;10(10):762. doi:10.1038/s41419-019-2008-0
18. Garcia-Dominguez M, Aguirre A, Lastra A, Hidalgo A, Baamonde A, Menendez L. The Systemic Administration of the Chemokine CCL1 Evokes Thermal Analgesia in Mice Through the Activation of the Endocannabinoid System. *Cell Mol Neurobiol*. 2019;39(8):1115–1124. doi:10.1007/s10571-019-00706-3
19. Wu Y-S, Chen S-N. Extracted Triterpenes from Antrodia cinnamomea Reduce the Inflammation to Promote the Wound Healing via the STZ Inducing Hyperglycemia-Diabetes Mice Model. *Front Pharmacol*. 2016;7:154. doi:10.3389/fphar.2016.00154
20. Kim HO, Cho SI, Chung BY, Ahn HK, Park CW, Lee CH. Expression of CCL1 and CCL18 in atopic dermatitis and psoriasis. *Clin Exp Dermatol*. 2012;37(5):521–526. doi:10.1111/j.1365-2230.2011.04295.x
21. He L, Zhu C, Jia J, et al. ADSC-Exos containing MALAT1 promotes wound healing by targeting miR-124 through activating Wnt/β-catenin pathway. *Biosci Rep*. 2020;40(5):5. doi:10.1042/BSR20192549
22. Zhao G, Liu F, Liu Z, et al. MSC-derived exosomes attenuate cell death through suppressing AIF nucleus translocation and enhance cutaneous wound healing. *Stem Cell Res Ther*. 2020;11(1):174. doi:10.1186/s13287-020-01616-8
23. Esposito D, Overall J, Grace MH, Komarnytsky S, Lila MA. Alaskan Berry Extracts Promote Dermal Wound Repair Through Modulation of Bioenergetics and Integrin Signaling. *Front Pharmacol*. 2019;10:1058. doi:10.3389/fphar.2019.01058
24. Long M, Rojo de la Vega M, Wen Q. Rojo de la Vega M, Wen Q, et al. An Essential Role of NRF2 in Diabetic Wound Healing. *Diabetes*. 2016;65(3):780–793. doi:10.2337/db15-0564
25. Xiao W, Tang H, Wu M, et al. Ozone oil promotes wound healing by increasing the migration of fibroblasts via PI3K/Akt/mTOR signaling pathway. *Biosci Rep*. 2017;37(6):6. doi:10.1042/BSR20170658
26. Park -H-H, Park N-Y, Kim S-G, Jeong K-T, Lee E-J, Lee E. Potential Wound Healing Activities of Galla Rhois in Human Fibroblasts and Keratinocytes. *Am J Chin Med*. 2015;43(8):1625–1636. doi:10.1142/S0192415X15500925
27. Pitz Hda S, Pereira A, Blasius MB, et al. In Vitro Evaluation of the Antioxidant Activity and Wound Healing Properties of Jaboticaba (Plinia peruviana) Fruit Peel Hydroalcoholic Extract. *Oxid Med Cell Longev*. 2016;2016:3403586. doi:10.1155/2016/3403586

28. Zhou ZQ, Chen Y, Chai M, et al. Adipose extracellular matrix promotes skin wound healing by inducing the differentiation of adipose-derived stem cells into fibroblasts. *Int J Mol Med*. 2019;43(2):890–900. doi:10.3892/ijmm.2018.4006
29. Takzaree N, Hadjiakhondi A, Hassanzadeh G, Rouini MR, Manayi A, Zolbin MM. Transforming growth factor-β (TGF-β) activation in cutaneous wounds after topical application of aloe vera gel. *Can J Physiol Pharmacol*. 2016;94(12):1285–1290. doi:10.1139/cjpp-2015-0460
30. Yang L, Zheng Z, Zhou Q, et al. miR-155 promotes cutaneous wound healing through enhanced keratinocytes migration by MMP-2. *J Mol Histol*. 2017;48(2):147–155. doi:10.1007/s10735-017-9713-8
31. Suga H, Sugaya M, Miyagaki T, et al. Association of nerve growth factor, chemokine (C-C motif) ligands and immunoglobulin E with pruritus in cutaneous T-cell lymphoma. *Acta Derm Venereol*. 2013;93(2):144–149. doi:10.2340/00015555-1428
32. Li Z, Chan K, Qi Y, et al. Participation of CCL1 in Snail-Positive Fibroblasts in Colorectal Cancer Contribute to 5-Fluorouracil/Paclitaxel Chemoresistance. *Cancer Res Treat*. 2018;50(3):894–907. doi:10.4143/crt.2017.356
33. Xu H, Liu X, Ni H. Clinical significance of miR-19b-3p in patients with sepsis and its regulatory role in the LPS-induced inflammatory response. *European Journal of Medical Research*. 2020;25(1):9. doi:10.1186/s40001-020-00408-3
34. Guo C, Liu J, Hao P, et al. The Potential Inhibitory Effects of miR-19b on Ocular Inflammation are Mediated Upstream of the JAK/STAT Pathway in a Murine Model of Allergic Conjunctivitis. *Invest Ophthalmol Vis Sci*. 2020;61(3):8. doi:10.1167/iovs.61.3.8
35. Lim J-Y, Ryu D-B, Lee S-E, Park G, Min C-K, Lim JY, Ryu DB, Lee SE, Park G, Min CK. Mesenchymal Stem Cells (MSCs). Mesenchymal Stem Cells (MSCs) Attenuate Cutaneous Sclerodermatous Graft-Versus-Host Disease (Scl-GVHD) through Inhibition of Immune Cell Infiltration in a Mouse Model. *J Invest Dermatol*. 2017;137(9):1895–1904. doi:10.1016/j.jid.2017.02.986
36. Chang R, Yi S, Tan X, et al. MicroRNA-20a-5p suppresses IL-17 production by targeting OSM and CCL1 in patients with Vogt-Koyanagi-Harada disease. *Br J Ophthalmol*. 2018;102(2):282–290. doi:10.1136/bjophthalmol-2017-311079
37. Ma T, Fu B, Yang X, Xiao Y, Pan M. Adipose mesenchymal stem cell-derived exosomes promote cell proliferation, migration, and inhibit cell apoptosis via Wnt/β-catenin signaling in cutaneous wound healing. *J Cell Biochem*. 2019;120(6):10847–10854. doi:10.1002/jcb.28376
38. Xu G, Ao R, Zhi Z, Jia J, Yu B. miR-21 and miR-19b delivered by hMSC-derived EVs regulate the apoptosis and differentiation of neurons in patients with spinal cord injury. *J Cell Physiol*. 2019;234(7):10205–10217. doi:10.1002/jcp.27690
39. Tang Y, Zhang Y-C, Chen Y, Xiang Y, Shen C-X, Li Y-G. The role of miR-19b in the inhibition of endothelial cell apoptosis and its relationship with coronary artery disease. *Sci Rep*. 2015;5(1):15132. doi:10.1038/srep15132
40. Qin D-N, Qian L, Hu D-L, et al. Effects of miR-19b Overexpression on Proliferation, Differentiation, Apoptosis and Wnt/β-Catenin Signaling Pathway in P19 Cell Model of Cardiac Differentiation In Vitro. *Cell Biochem Biophys*. 2013;66(3):709–722. doi:10.1007/s12013-013-9516-9
41. Liu WG, Han LL, Xiang R. Protection of miR-19b in hypoxia/reoxygenation-induced injury by targeting PTEN. *J Cell Physiol*. 2019. doi:10.1002/jcp.28286
42. Li Z, Cai J, Cao X. MiR-19 suppresses fibroblast-like synoviocytes cytokine release by targeting toll like receptor 2 in rheumatoid arthritis. *Am J Transl Res*. 2016;8(12):5512–5518.
43. Luo X-Q, Shao J-B, Xie R-D, et al. Micro RNA-19a interferes with IL-10 expression in peripheral dendritic cells of patients with nasal polyposis. *Oncotarget*. 2017;8(30):48915–48921. doi:10.18632/oncotarget.16555